Peer-reviewed version available at Polymers 2018, 10, 676; doi:10.3390/polym10060676

Article

Critical Point Drying: An Effective Tool for Direct Measurement of the Surface Area of Pretreated Cellulosic Biomass

Kyu-Young Kang [1], Kyung Ran Hwang [2], Ji-Yeon Park [2], Joon-Pyo Lee [3], Jun-Seok Kim [4] and Jin-Suk Lee [3,*]

[1] Department of Biological and Environmental Science, Dongguk University-Seoul, 32 Dongguk-ro, Ilsandong-gu, Goyang 10326, Korea; kykang@dongguk.edu (K.-Y.K.)
[2] Biomass and Waste Energy Laboratory, Korea Institute of Energy Research, 152 Gajeong-ro, Yuseong-gu, Daejeon 34129, Korea; hkran@kier.re.kr (K.R.H.); yearn@kier.re.kr (J.-Y.P.)
[3] Gwangju Bioenergy R&D Center, Korea Institute of Energy Research, 25 Samso-ro270beongil, Buk-gu, Gwangju 61003, Korea; bmjplee@kier.re.kr (J.-P.L.)
[4] Department of Chemical Engineering, Kyonggi University, 154-42 Gwanggyosan-ro, Yeongtong-gu, Suwon 16227, Korea; jskim84@kyonggi.ac.kr (J.-S.K.)
* Correspondence: bmjslee@kier.re.kr; Tel.: +82-62-717-2410

Abstract: Surface area and pore size distribution of *Eucalyptus* samples pretreated by different methods were determined by the Brunauer-Emmett-Teller (BET) technique. Three methods were applied to prepare cellulosic biomass samples for BET measurements: air, freeze, and critical point drying (CPD). Air and freeze drying caused severe collapse of biomass pore structures, but CPD effectively preserved biomass morphology. Surface area of CPD prepared *Eucalyptus* samples was determined to be 58–161 m^2/g, whereas air and freeze dried samples were 0.5–1.3 and 1.0–2.4 m^2/g, respectively. Average pore diameter of CPD prepared *Eucalyptus* samples were 61–70Å. CPD preserved *Eucalyptus* sample morphology by replacing water with a non-polar solvent, CO_2 fluid, which prevented hydrogen bond reformation in the cellulose.

Keywords: pretreated cellulosic biomass; critical point drying; surface area; pore size distribution; Brunauer-Emmett-Teller; cellulose; hornification

1. Introduction

For efficient sugar fractionation from lignocellulosic biomass, physical contact between cellulose and cellulase enzymes is necessary. Therefore, cellulose specific surface area available for enzyme contact is one of the most important factors determining the rate and extent of enzymatic hydrolysis of biomass [1–3]. Since the average size of cellulase enzymes is approximately 5.1 nm, internal surface of pores greater than 5.1 nm should be particularly effective for enzymatic hydrolysis [4]. Various pretreatments applied for improved enzymatic digestibility also increase surface area, due not only to removal of hemicellulose and/or lignin, but also cellulose swelling. Most studies regarding biomass specific surface area and pore size distribution have employed indirect measurement techniques such as solute exclusion [5–8], non-hydrolytic protein adsorption [9] Simons' staining [10–12], and NMR techniques [13–14].

Solute exclusion is the most widely employed method, but has several drawbacks, including relatively low accuracy and limitations on pore size ranges that can be determined. For example, given the unavailability of dextran molecule probes, only pore sizes up to 56 nm can be measured [5–7,15]. However, non-ionic surfactant pretreatment of lignocellulosic biomass can produce pores up to 100 nm diameter [16]. Inaccurate estimation can also arise from the water competition with the

solute probes [1] and/or solute concentration measurement errors. Reported biomass surface area varies greatly, from 20 to over 1,500 m^2/g [7,15].

Simons' staining method has also been used to determine the feasibility of enzymatic hydrolysis of substrates [10–12,17], although this technique can provide only semi-quantitative information. It also has similar limitations to solute exclusion, since it also employs dye solutes for the measurement. In the other hand, NMR techniques employed for biomass surface area measurement require complicated experiment set-ups [13–14].

The Brunauer-Emmett-Teller (BET) technique employing N_2 adsorption has many advantages, including high accuracy and can measure 0.4–300 nm pore sizes [18]. Therefore, the BET technique is widely used to determine surface area and pore size distribution of porous materials, although it is applicable only to dried samples. Few studies have considered BET based internal surface area measurement of pretreated biomass [11,19,20]. However, these indicate that BET measured surface areas differ significantly from those measured by other methods, i.e. solute exclusion, dye staining, or probes. For example, Wiman *et al*. compared steam pretreated spruce surface area by BET and Simmons' staining methods [11]. BET measurement biomass samples were oven dried at 30°C for 24 hours to minimize structural changes. Pretreated biomass surface area was 1.3–8.2 m^2/g, far smaller than those measured by the staining method (53–64 m^2/g). The small BET based surface area was attributed mainly to pore collapse during air drying [12,21].

To avoid pore collapse, freeze drying has been applied to cellulose and yellow poplar (*Liriodendron tulipifera*) wood flour pretreated by organosolv process [19,20], but the biomass surface area remains small, 5–39 and 1.8 m^2/g for cellulose and organosolv pretreated yellow poplar, respectively. Esteghalian *et al*. investigated the effects of drying conditions on enzymatic hydrolysis of Douglas fir (*Pseudotsuga menziesii*) kraft pulp using air, oven, and freeze drying; and compared dried biomass enzymatic digestibilities. No significant differences between air and freeze dried biomass samples were evident [17]. Thus, there remains no successful method that prevents pore collapse when drying cellulosic biomass. Therefore, cellulosic biomass surface area is mainly determined by *in situ* measuring techniques.

Critical point drying (CPD) is widely used to dry delicate samples for Scanning Electron Microscope (SEM) applications and could be a viable option for biomass sample preparation, while maintaining the original morphology. Since pore collapse is caused by removal of water, a polar solvent, from the biomass [12,21], this study attempted to prevent pore collapse by replacing water with non-polar solvents before drying. Since CPD employing a non-polar solvent (liquid CO_2) is done at ~36°C, deterioration caused by high drying temperature can be minimized. There have been no previous reports on direct measurement of surface area and/or pore size distribution for CPD pretreated cellulosic biomass.

This study prepared *Eucalyptus* wood flour samples using three pretreatment methods to measure total surface area and pore size distribution, and drying conditions effects on surface area and pore size distribution were compared. This work will contribute to deeper understanding of the physical effects of surface area and pore size distribution on enzymatic hydrolysis rates of cellulosic biomass.

2. Materials and Methods

2.1. Materials

Eucalyptus (*E. grandis*) wood chips were supplied by Dr. Zhuang of GuangZhou Institute of Energy Conversion, Chinese Academy of Science (GIEC) in China, knife milled by Wiley mill (Mini Wiley mill, Thomas Scientific, Swedesboro, NJ, USA) and screened to a nominal size of 20–60 mesh. Alkaline electrolyzed water (ALEW) was provided by Gendocs Inc. (Daejeon, Korea) with pH = 12.2 and ORP < –795 mV. All other reagents and chemicals were analytical grade and purchased from either Sigma–Aldrich (St. Louis, MO, USA) or local suppliers in Korea.

2.2. Pretreatments of Lignocellulosic biomass

Eucalyptus samples as lignocellulosic biomass were pretreated by dilute acid (DA), steam after NaOH impregnation, and ALEW. For DA pretreatment, 60 g (OD) of biomass sample was immersed in 160 mL of 3% (w/w) sulfuric acid and maintained at 121°C for 2 h. The slurry was allowed to stand overnight and then filtered (Whatman No. 1 glass filter) to recover insoluble solids. The recovered cellulosic biomass was washed with distilled water several times. The process of NaOH–steam pretreatment followed the procedure detailed previously [22]. 60 g (OD) of biomass sample was soaked in 480 mL of 3% (w/v) sodium hydroxide solution at room temperature. The slurry was allowed to stand overnight and then filtered (Whatman No. 1 glass filter) to recover insoluble solids. The recovered solids were transferred to an autoclave (working volume = 1 L) and steam pretreatment was conducted at 160°C for 12 min under 20 bar nitrogen atmosphere. For ALEW pretreatment, 60 g (OD) of biomass sample was immersed in 600 mL ALEW and maintained at 180°C for 1 h in an autoclave (working volume = 1 L) under 20 bar nitrogen atmosphere.

2.3. Drying of cellulosic biomass sample

The pretreated samples were dried by air, freeze, and critical point drying methods. For air drying (AD), approximately 5 g of each pretreated cellulosic biomass samples was dried in a vacuum oven at 50°C for 48 h. Constant weight was confirmed after drying. The freeze drying (FD) process of cellulosic biomass sample followed that detailed in the literature [19]. Approximately 5 g of pretreated cellulosic biomass sample was frozen at –60°C for 48 h, and then vacuumed in a FD apparatus for 72 h. Critical point drying (CPD) was performed using a critical point dryer (13200J–AB, SPI Supplies, West Chester, PA, USA), following the procedure provided in the operation manual. Approximately 5 g of pretreated biomass samples were placed in 100 mL of 30, 50, 70, 90, 95 and 100% ethanol for 15 min, then immersed in acetone solution for a further 15 min. After a series of solvent exchanges, acetone in the samples became replaced by liquid CO_2, and the samples were then critical point dried at 36°C.

2.4. Surface area and pore size measurements of biomass sample

We used the BET method to determine surface area, average pore diameter, and total pore volume for AD, FD, and CPD biomass samples. N_2 adsorption was measured using an accelerated surface area and porosity analyzer (ASAP 2420, Micromeritics Inc., Norcross, GA, USA). N_2 adsorption isotherms were obtained by measuring the amount of gas adsorbed across a range of relative pressures (P/P_0) at constant temperature (–196°C, liquid nitrogen phase temperature), where P and P_0 are the equilibrium and saturation pressures of adsorbate gas at the temperature of adsorption, respectively. Desorption isotherms were achieved by measuring the amount of N_2 gas removed as pressure decreased. Subsequently the specific surface area was calculated from the adsorption isotherms using BET theory. Total pore volume was estimated from the amount of N_2 gas adsorbed at 0.98 relative pressure, under the following assumptions: pores were filled with liquid nitrogen, and adsorption average pore size was derived from $4V/A$, where V is the total pore volume, and A is the surface area, corresponding to the assumed cylindrical pore model. Pore size distribution was obtained from experimental isotherms as detailed elsewhere [24]. Prior to BET analysis, pre-dried samples were degassed at 90°C for 0.5 h and then again at 105°C for 4 h.

2.5. FT–IR analysis

Structural changes of raw and pretreated samples were examined with Fourier transform infrared spectroscopy (FT–IR). The samples were ground into powder and sieved through 149 μm mesh. FT–IR spectra were recorded on an FTS–175C (Bio-Rad Laboratories Inc., Hercules, CA, USA) equipped with mercury cadmium telluride detector, using KBr pellets. All spectra were collected at 4 cm^{-1} resolution with 32 scans in the range 4000–500 cm^{-1}.

3. Results and Discussion

3.1. Drying methods effects on surface area and pore size distribution of pretreated Eucalyptus

Surface area and pore size distribution of sample were determined by BET and the differences were compared among CPD, AD, and FD pretreatments. Figure 1 shows N_2 adsorption–desorption isotherms for ALEW, DA, and NaOH–steam pretreated samples. The isotherms are typical type IV hysteresis loops (as classified by IUPAC), consistent with mesoporous materials where an adsorbate monolayer is formed on the pore surface at low pressures followed by multilayer formation. The hysteresis loop originates from capillary condensation in meso and macropores, and can have a wide variety of shapes depending on the pore geometries. Specific pore structures can often be identified from their hysteresis loop shape based on the empirical IUPAC classification. AD and FD samples also exhibited H4 type hysteresis loops, although somewhat smaller. This hysteresis type is consistent with narrow slit shaped pores and/or aggregated particles [25]. All CPD samples exhibited H2 type hysteresis loops, where pore size and pore shape distribution are not well-defined, i.e., irregular. The desorption isotherm steep slope, observed for all CPD samples, typically indicates pore interconnection [26].

Figure 2 shows the corresponding biomass pore size distribution, determined by the BJH method. As reported elsewhere, AD and FD samples' large pores indicate collapse of most small pore structures during drying [26]. However, CPD appears to maintain the micropore structures in the pretreated *Eucalyptus* samples, with average pore size approximately 6.2 nm, i.e., within the mesopore range.

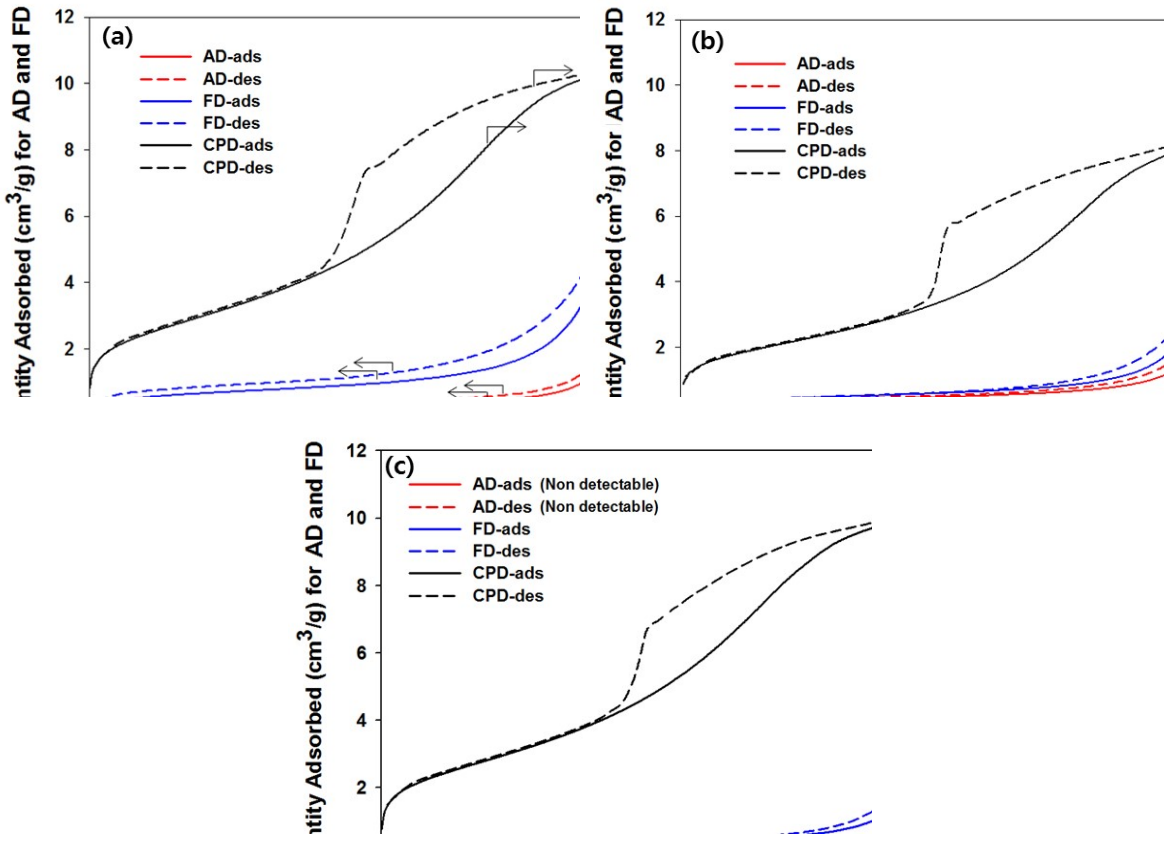

Figure 1. Nitrogen adsorption–desorption isotherms for air (AD), freeze (FD), and critical point (CPD) dried *Eucalyptus* samples with (a) ALEW, (b) 1% H_2SO_4, (c) NaOH–steam pretreatments.

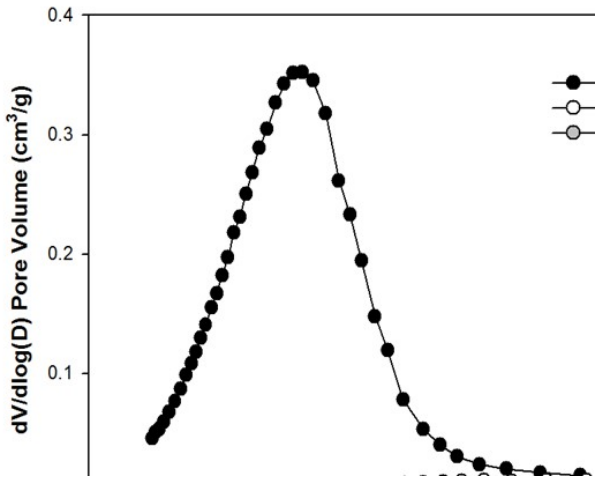

Figure 2. Drying method effects on pore size distribution for ALEW pretreated *Eucalyptus* samples.

Table 1 shows detailed quantitative data for the ALEW pretreated *Eucalyptus* samples. Surface area of pretreated *Eucalyptus* sample varied greatly with the drying conditions. The smallest surface areas were from AD samples (0.5–1.3 m^2/g), with FD samples having approximately twice the area (1.04–2.44 m^2/g), although they had comparable small pore volumes (0.002–0.005 and 0.005–0.015 cm^3/g, respectively); whereas CPD sample surface area and pore volume were considerably larger (58.5–161.5 m^2/g and 0.103–0.249 cm^3/g, respectively).

Surface area of AD *Eucalyptus* samples was somewhat smaller than previously reported for SO_2–steam pretreated spruce (1.3–8.2 m^2/g) [11], which is possibly due to the different feedstocks and pretreatment conditions. However, surface area of SO_2–steam pretreated spruce varied greatly with pretreatment conditions tested in that study. The surface area of FD *Eucalyptus* samples was comparable to previously reported for yellow poplar (*L. tulipifera*) (1.80 m^2/g) prepared by FD after organosolv pretreatment [20]. Table 3 compares surface areas of CPD *Eucalyptus* sample with those previously reported. The CPD surface area for DA pretreated *Eucalyptus* (57.3 m^2/g) was very close to SO_2–steam pretreated spruce determined by dye staining (58.5 m^2/g) [11].

Thus, only CPD effectively maintained the pretreated biomass morphology, although both of FD and CPD have been previously reported as effective. Both drying methods have been widely employed in SEM specimen preparation [27]. The poor performance of FD for water-swollen lignocellulose reported here is probably associated with the cellulose content of feedstock, since cellulose is deformed by hornification, a consequence of irreversible changes to the cell wall structure [12].

Table 1. Mean surface areas, pore diameters and total pore volumes for ALEW pretreated *Eucalyptus* samples.

Pretreatment	Drying method	Surface area (m^2/g)	Average pore diameter (Å)	Total pore volume (cm^3/g)
ALEW	AD[1]	0.9	–	0.005
	FD[2]	2.4	–	0.015
	CPD[3]	161.5	61.7	0.249

[1] Air drying. [2] Freeze drying. [3] Critical point drying.

Table 2. Drying method effect on BET surface area.

Biomass	Drying condition	Surface area (m^2/g)	Reference
Spruce [1]	Air drying at 30°C	6.3	[11]
Yellow poplar [2]	Freeze drying	1.8	[20]
Eucalyptus [3]	Critical point drying	58.5	Current paper

[1] Pretreated by 2.5% SO_2 at 207°C for 7 min. [2] Pretreated by EtOH (organosolv) at 130°C for 50 min.
[3] Pretreated by 1% H_2SO_4 at 121°C for 2 h.

Table 3. Comparison of BET results with those determined by non-drying measurement techniques.

Biomass	Measurement technique	Surface area (m^2/g)	Surface area accessible to cellulose (m^2/g)	Reference
Corn cob	Solute exclusion	–	57.4 [1] 34.1 [2]	[7]
	Protein adsorption	–	7.7 [3]	[32]
Lodgepole pine pulp [4]	Solute exclusion	–	22.4	[8]
Mixed hard wood [5]	Solute exclusion	1,134	25.8	[15]
Filter paper	Protein adsorption	–	9.8	[9]
Spruce [6]	Dye staining	57.3	–	[11]
Eucalyptus [7]	BET	58.5	–	Current paper

[1] Pretreated by 2% NaOH at 80°C for 6 h. [2] Pretreated by 2% H_2SO_4 at 120°C for 0.75 h.
[3] Pretreated by 0.048g H_2SO_4/g biomass at 190°C for 1 min. [4] Pretreated by SPORL at 180°C for 20 min.
[5] Pretreated by 1% H_2SO_4 at 180°C for 8.3 s. [6] Pretreated by 2.5% SO_2 at 207°C for 7 min.
[7] Pretreated by 1% H_2SO_4 at 121°C for 2 h.

Although the exact hornification mechanism is unclear, one possible explanation is hydrogen bond breaking and reforming corresponding to cellulose wetting and drying, respectively. When cellulose is wet, fibers swell by hydrogen bond breakage, but shrink with reforming of hydrogen bonds upon drying. In any case, the reason for the poor FD performance remains unknown. Possibly FD removes only free water, but not the bound water, inducing cellulosic collapse [28]. However, hydrogen reforming could be prevented if the bound water in pretreated *Eucalyptus* samples was replaced by a non-polar solvent prior to drying. To examine this hypothesis, we performed an FT–IR analysis to examine the hydrogen bonds in ALEW pretreated AD and CPD *Eucalyptus* samples, as shown in Figure 3.

The –OH stretching region of the FT–IR absorbance band, 3000–4000 cm^{-1}, is reported to contain information on hydrogen bonding in cellulose [29,30], and large peaks were observed between 3340–3380 cm^{-1}. ALEW pretreated CPD *Eucalyptus* sample peaks are significantly smaller than those of untreated and ALEW pretreated AD *Eucalyptus*. AD *Eucalyptus* peak height was very similar to that of untreated *Eucalyptus*. Thus, since peak height is proportional to hydrogen bonds in the biomass sample, CPD *Eucalyptus* had significantly fewer hydrogen bonds than untreated or AD *Eucalyptus*. Overall, hydrogen bonds in untreated *Eucalyptus* were broken by water during pretreatment and subsequently reconnected upon AD. However, hydrogen bond reformation upon drying was successfully prevented for CPD *Eucalyptus* samples, replacing bound water with a non-polar solvent, liquid CO_2, prior to drying. Finally, the wide peak at 3388.9 cm^{-1} shifted to higher frequency after drying of ALEW pretreated *Eucalyptus*. This shift was more significant with AD, where hydrogen bonding became stronger than was the case for untreated sample.

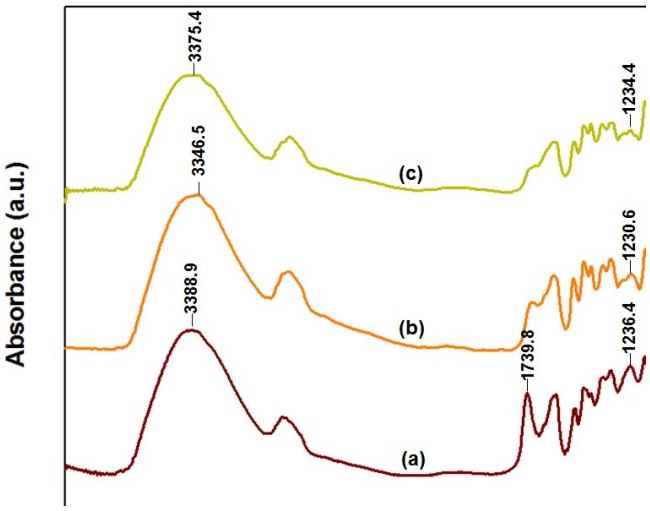

Figure 3. FT-IR spectra for dried *Eucalyptus* samples before and after ALEW: (a) untreated control, (b) air drying (AD) after ALEW, (c) critical point drying (CPD) after ALEW.

3.2. Pretreatment conditions effects on surface area and pore size distribution

Since pore volumes varied sharply with pretreatment methods (Figure 4), we investigated pretreatment condition influences on pore volumes, surface area, and pore size distribution for CPD *Eucalyptus* samples. Alkali pretreatment yielded biomass with higher pore volume and surface area than those achieved by acid pretreatment. Swelling effects of alkali pretreatment have been reported previously. Huang *et al*. showed that NaOH pretreated corn cob had approximately 40% larger surface area (57.4 m^2/g) than the corresponding sulfuric acid pretreated sample [7]. In the current study, the ALEW pretreatment exhibited the strongest swelling effect on *Eucalyptus* samples with approximately 20% higher pore volume but similar average pore size, hence approximately 20% larger surface area than NaOH–steam pretreatment.

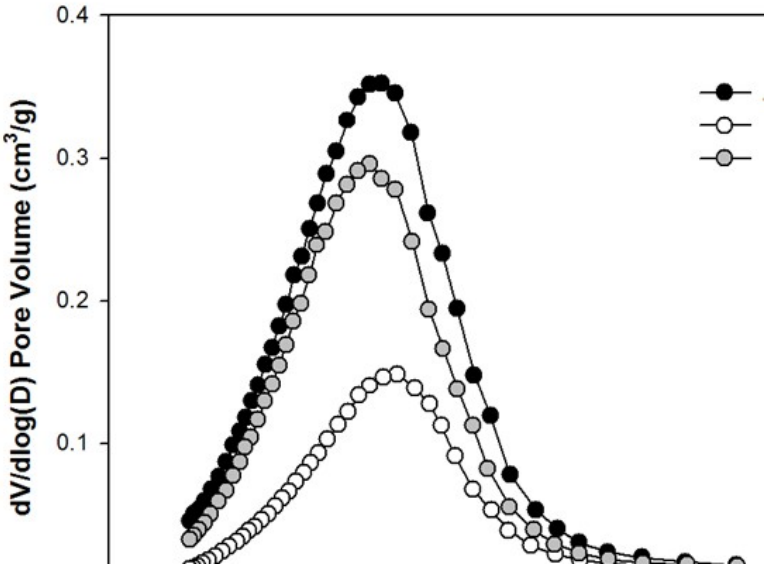

Figure 4. Pretreatment method effects on pore size distribution for ALEW critical point dried *Eucalyptus* samples.

Table 4 summarizes the effects of these and the other quantified pretreatment on pore volume and surface area of *Eucalyptus* samples. DA pretreatment exhibits lowest pore volume and smallest surface area, approximately 45% of the values from NaOH pretreated *Eucalyptus* samples. The reason for the smaller surface area with DA pretreatment is unclear, although it is likely due to cellulose aggregation [7].

Biomass pore volume and surface area provide enzymes with sufficient access and adsorption to cell surfaces, thus significantly affecting enzymatic hydrolysis of cellulose. Therefore, we determined pore volumes for the different pore sizes, as shown in Table 5. ALEW pretreated *Eucalyptus* samples exhibited the largest pore volume accessible to enzymes, with NaOH pretreated samples exhibiting the highest pore volumes for pores smaller than 2 nm and ALEW pretreated samples having the highest pore volumes for larger pore sizes. The 25% larger surface area of ALEW pretreated samples is remarkable, even after considering the higher pore volume for larger than 2 nm pores. This larger surface area is probably due to the high lignin content, since most lignin micropores are smaller than 0.6 nm [31].

Table 4. Effects of pretreatment conditions on surface areas, average pore sizes and pore volumes of CPD *Eucalyptus* samples.

Pretreatment	Surface area (m^2/g)	Average pore diameter (Å)	Total pore volume (cm^3/g)
Untreated	0.8	34.1	0.007
ALEW[1]	161.5	61.7	0.249
DA[2]	58.5	70.6	0.103
NaOH–steam[3]	129.9	62.1	0.202

[1] Pretreated by alkali electrolyzed water (ALEW) at 180°C for 1 h. [2] Pretreated by 1% H_2SO_4 at 121°C for 2 h. [3] Pretreated by steam at 160°C for 12 min after 3% NaOH soaking for 12 h.

Table 5. Effects of pretreatment conditions on micropore volumes of *Eucalyptus* samples.

Pretreatment	Pore diameter (nm)			
	$P_d < 2$	$2 < P_d < 5$	$5 < P_d$	Total
ALEW	0.019	0.08	0.15 (60%)*	0.249
1% H_2SO_4	0.003	0.03	0.07 (68%)	0.103
NaOH–steam	0.022	0.06	0.12 (59%)	0.202

* Pore volume fraction.

4. Conclusions

Critical point drying was shown to effectively prevent cellulosic pore collapse upon drying and hence enable direct determination of specific surface area and pore size distribution for pretreated *Eucalyptus* samples using the BET method. Comparing hydrogen bonds for the various drying methods, reformation of hydrogen bonds upon drying is mainly responsible for pore collapse. Thus, hydrogen bond reformation was successfully prevented in CPD by replacing water with liquid CO_2, a non-polar solvent, before drying.

The measurement technology developed in this study will provide more detailed quantitative data on surface area and pore size distribution of water-swollen biomass.

Surface areas of CPD *Eucalyptus* samples were 58–161 m^2/g, comparable to those determined by indirect measuring methods; whereas sulfuric acid pretreatment yielded considerably smaller surface area with larger average pore diameter, ALEW pretreatment produced the highest surface area, and NaOH steam pretreatment produced somewhat smaller surface area.

Acknowledgments: This work was supported by International Collaborative R&D grant (No. 20138520091130) of the Korea Institute of Energy Technology Evaluation and Planning (KETEP) funded by the Korea Government Ministry of Trade, Industry and Energy. This study was also supported by the research program of Dongguk University, 2017 (S–2017–G0001–00046).

Author Contributions: K.R. Hwang and J.-S. Lee conceived and designed the experiments; J.-Y. Park and J.-P. Lee performed the experiments; K.-Y. Kang and J.-S. Kim analyzed the data; K.-Y. Kang and J.-S. Lee wrote the paper.

References

1. Zhao, X.; Zhang, L.; Liu, D. Biomass recalcitrance. Part 1: the chemical compositions and physical structures affecting the enzymatic hydrolysis of lignocellulose. *Biofuels, Bioprod. Bioref.* **2012**, *6(4)*, 465–482, DOI: 10.1002/bbb.1331.
2. Mood, S.H.; Golfeshan, A.H.; Tabatabaei, M.; Jouzani, G.S.; Najafi, G.H.; Gholami, M.; Ardjmand, M. Lignocellulosic biomass to bioethanol, a comprehensive review with a focus on pretreatment. *Ren. Sustain. Energy Rev.* **2013**, *27*, 77–93, DOI: 10.1016/j.rser.2013.06.033.
3. Meng, X.; Ragauskas, A.J. Recent advances in understanding the role of cellulose accessibility in enzymatic hydrolysis of lignocellulosic substrates. *Curr. Opin. Biotechnol.* **2014**, *27*, 150–158, DOI: 10.1016/j.copbio.2014.01.014.
4. Grethlein, H.E. The effect of pore size distribution on the rate of enzymatic hydrolysis of cellulosic substrates. *Nat. Biotechnol.* **1985**, *3*, 155–160, DOI: 10.1038/nbt0285-155.
5. Stone, J.E.; Scallan, A.M. A structural model of the cell wall of water-swollen wood pulp fibers based on their accessibility to macromolecules. *Cellul. Chem. Technol.* **1968**, *2(3)*, 321–342.
6. Gama, F.M.; Teixeira, J.A.; Mota, M. Cellulose morphology and enzymatic reactivity: A modified solute exclusion technique. *Biotechnol. Bioeng.* **1994**, *43(5)*, 381–387, DOI: 10.1002/bit.260430506.
7. Huang, R.; Su, R.; Qi, W.; He, Z. Understanding the key factors for enzymatic conversion of pretreated lignocellulose by partial least square analysis. *Biotechnol. Prog.* **2010**, *26(2)*, 384–392, DOI: 10.1002/btpr.324.
8. Wang, W.; Liu, P.; Zhang, M.; Hu, J.; Xing, F. The pore structure of phosphoaluminate cement. *J. Compos. Mater.* **2012**, *2(3)*, 104–112, DOI: 10.4236/ojcm.2012.23012.
9. Hong, J.; Ye, X.; Zhang, Y.H. Quantitative determination of cellulose accessibility to cellulase based on adsorption of a nonhydrolytic fusion protein containing CBM and GFP with its applications. *Langmuir* **2007**, *23(25)*, 12535–12540, DOI: 10.1021/la7025686.
10. Del Rio, L.F; Chandra, R.P.; Saddler, J.N. The effects of increasing swelling and anionic charges on the enzymatic hydrolysis of organosolv–pretreated softwoods at low enzyme loadings. *Biotechnol. Bioeng.* **2011**, *108(7)*, 1549–1558, DOI: 10.1002/bit.23090.
11. Wiman, M.; Dienes, D.; Hansen, M.A.T.; van der Meulen, T.; Zacchi, G.; Lidén, G. Cellulose accessibility determines the rate of enzymatic hydrolysis of steam–pretreated spruce. *Bioresour. Technol.* **2012**, *126*, 208–215, DOI: 10.1016/j.biotech.2012.08.082.
12. Luo, X.; Zhu, J.Y. Effects of drying–induced fiber hornification on enzymatic saccharification of lignocelluloses. *Enz. Microb. Technol.* **2011**, *48(1)*, 92–99, DOI: 10.1016/j.enzmictec.2010.09.014.
13. Foston, M.; Ragauskas, A.J. Changes in the structure of the cellulose fiber wall during dilute acid pretreatment in *Populus* studied by ^{1}H and ^{2}H NMR. *Energy Fuels* **2010**, *24(10)*, 5677–5685, DOI: 10.1021/ef100882t.
14. Meng, X.; Foston, M.; Leisen, J.; DeMartini, J.; Wyman, C.E.; Ragauskas, A.J. Determination of porosity of lignocellulosic biomass before and after pretreatment by using Simons' stain and NMR techniques. *Bioresour. Technol.* **2013**, *144*, 467–476, DOI: 10.1016/j.biotech.2013.06.091.
15. Thompson, D.N.; Chen, H.-C.; Grethlein, H.E. Comparison of pretreatment methods on the basis of available surface area. *Bioresour. Technol.* **1992**, *39(2)*, 155–163, DOI: 10.1016/0960-8524(92)90135-K.
16. Seo, D.-J.; Fujita, H.; Sakoda, A. Structural changes of lignocelluloses by a nonionic surfactant, Tween 20, and their effects on cellulase adsorption and saccharification. *Bioresour. Technol.* **2011**, *102(20)*, 9605–9612, DOI: 10.1016/j.biotech.2011.07.034.
17. Esteghlalian, A.R.; Bilodeau, M.; Mansfield, S.D.; Saddler, J.N. Do enzymatic hydrolyzability and Simons' stain reflect the changes in the accessibility of lignocellulosic substrates to cellulase enzymes? *Biotechnol. Prog.* **2001**, *17(6)*, 1049–1054, DOI: 10.1021/bp0101177.

18. Allen, T. Surface area and pore size determination. In *Particle Size Measurement*, 5th ed.; Allen, T., Eds.; Springer/Chapmann & Hall: London, UK, 1997; Volume 2, pp. 44–108, ISBN 978-0-412-75330-5.
19. Guo, J.; Catchmark, J.M. Surface area and porosity of acid hydrolyzed cellulose nanowhiskers and cellulose produced by *Gluconacetobacter xylinus*. *Carbohydr. Polym.* **2012**, *87(2)*, 1026–1037, DOI: 10.1016/j.carbpol.2011.07.060.
20. Koo, B.-W.; Min, B.-C.; Gwak, K.-S.; Lee, S.-M.; Choi, J.-W.; Yeo, H.; Choi, I.-G. Structural changes in lignin during organosolv pretreatment of *Liriodendron tulipifera* and the effect on enzymatic hydrolysis. *Biomass Bioenerg.* **2012**, *42*, 24–32, DOI: 10.1016/j.biombioe.2012.03.012.
21. Park, S.; Venditti, R.A.; Jameel, H.; Pawlak, J.J. Changes in pore size distribution during the drying of cellulose fibers as measured by differential scanning calorimetry. *Carbohydr. Polym.* **2006**, *66(1)*, 97–103, DOI: 10.1016/j.carbpol.2006.02.026.
22. Choi, W.-I.; Park, J.-Y.; Lee, J.-P.; Oh, Y.-K.; Park, Y.C.; Kim, J.S.; Park, J.M.; Kim, C.H.; Lee, J.-S. Optimization of NaOH–catalyzed steam pretreatment of empty fruit bunch. *Biotechnol. Biofuels*, **2013**, *6(170)*, 1–8, DOI: 10.1186/1754-6834-6-170.
23. NREL. Chemical Analysis and Testing Laboratory Analytical Procedures (CAT), Eds.; National Renewable Energy laboratory: Golden, CO, USA, 2004.
24. Barrett, E.P.; Joyner, L.G.; Halenda, P.P. The determination of pore volume and area distributions in porous substances. I. Computations from nitrogen isotherms. *J. Am. Chem. Soc.* **1951**, *73(1)*, 373–380, DOI: 10.1021/ja01145a126.
25. Sing, K.S.W.; Everett, D.H.; Haul, R.A.W.; Moscou, L.; Pierotti, R.A.; Rouquérol, J.; Siemieniewska, T. Reporting physisorption data for gas/solid systems with special reference to the determination of surface area and porosity. *Pure Appl. Chem.* **1985**, *57(4)*, 603–619, DOI: 10.1515/iupac.57.0007.
26. Mason, G. The effect of pore space connectivity on the hysteresis of capillary condensation in adsorption–desorption isotherms. *J. Colloid Interface Sci.* **1982**, *88(1)*, 36–46, DOI: 10.1016/0021-9797(82)90153-9.
27. Nordestgaard, B.G.; Rostgaard J. Critical–point drying versus freeze drying for scanning electron microscopy: a quantitative and qualitative study on isolated hepatocytes. *J. Microsc.* **1985**, *137*, 189–207.
28. Jie, X.; Cao, Y.; Qin, J.J.; Liu, J.; Yuan, Q. Influence of drying method on morphology and properties of asymmetric cellulose hollow fiber membrane. *J. Membrane Sci.* **2005**, *246(2)*, 157–165, DOI: 10.1016/j.memsci.2004.08.007.
29. Liu, W.; Hou, Y.; Wu, W.; Niu, M.; Wang, W. Pretreatment of wheat straw using SO_2 dissolved in hot water. *Bioresour. Technol.* **2012**, *124*, 306–310, DOI: 10.1016/j.biortech.2012.08.028.
30. Kawamoto, H.; Ueno, Y.; Saka, S. Thermal reactivities of non-reducing sugars in polyether–Role of intermolecular hydrogen bonding in pyrolysis. *J. Anal. Appl. Pyrol.* **2013**, *103*, 287–292, DOI: 10.1016/j.jaap.2012.08.009.
31. Nakatani, T.; Ishimaru, Y.; Iida, I.; Furuta, Y. Micropore structure of wood: Change in micropore structure accompanied by delignification. *J. Wood Sci.* **2008**, *54(3)*, 252–255, DOI: 10.1007/s10086-007-0931-7.
32. Zhu, Z.; Sathitsuksanoh, N.; Vinzant, T.; Schell, D.J.; McMillan, J.D.; Zhang, Y.-H.P. Comparative study of corn stover pretreated by dilute acid and cellulose solvent–based lignocellulose fractionation: Enzymatic hydrolysis, supramolecular structure, and substrate accessibility. *Biotechnol. Bioeng.* **2009**, *103(4)*, 715–724, DOI: 10.1002/bit.22307.